Geometrical Shape of Micelles Formed by Cationic Dimeric Surfactants Determined with Small-Angle Neutron Scattering

ARTICLE *in* LANGMUIR · MAY 2012

Impact Factor: 4.46 · DOI: 10.1021/la301190d · Source: PubMed

2 AUTHORS:

Magnus Bergstrom
Uppsala University
62 PUBLICATIONS **1,570** CITATIONS
SEE PROFILE

Vasil M Garamus
Helmholtz-Zentrum Geesthacht
223 PUBLICATIONS **2,547** CITATIONS
SEE PROFILE

Langmuir

Article

pubs.acs.org/Langmuir

Geometrical Shape of Micelles Formed by Cationic Dimeric Surfactants Determined with Small-Angle Neutron Scattering

L. Magnus Bergström*,[†] and Vasil M. Garamus[‡]

[†]School of Chemical Science and Engineering, Department of Chemistry, Surface and Corrosion Science, KTH Royal Institute of Technology, SE-100 44 Stockholm, Sweden

[‡]Helmholtz-Zentrum Geesthacht: Centre for Materials and Coastal Research, D-215 02 Geesthacht, Germany

Supporting Information

ABSTRACT: The influence of spacer group on the geometrical shape of micelles formed by quaternary-bis dimeric (Gemini) surfactants $C_{12}H_{25}N(CH_3)_2(CH_2)_sN(CH_3)_2C_{12}H_{25}$ (12-*s*-12) has been investigated with small-angle neutron scattering (SANS). Dimeric surfactants with a short spacer unit (12-3-12 and 12-4-12) are observed to form elongated general ellipsoidal micelles with half axes $a < b < c$, whereas SANS data demonstrate that 12-*s*-12 surfactants with $6 \leq s \leq 12$ form rather small spheroidal micelles rather than strictly spherical micelles. By means of comparing our present SANS results with previously determined growth rates using time-resolved fluorescence quenching, we are able to conclude that micelles formed by 12-6-12, 12-8-12, 12-10-12, and 12-12-12 are shaped as oblate rather than prolate spheroids. As a result, our present investigation suggests a never before reported structural behavior of Gemini surfactant micelles, according to which micelles transform from elongated ellipsoids to nonelongated oblate spheroids as the length of the spacer group is increased. The aggregation number of oblate micelles is observed to monotonously decrease with an increasing length of the surfactant spacer group, mainly as a result of a decreasing minor half axis (a), whereas the major half axis (b) is rather constant with respect to s. We argue that geometrically heterogeneous elongated micelles are formed by dimeric surfactants with a short spacer group mainly as a result of the surface charges becoming less uniformly distributed over the micelle interface. As the length of the spacer group increases, the distance between intramolecular charges become approximately equal to the average distance between charges on the micelle interface, and as a result, rather small oblate spheroidal micelles with a more uniform distribution of surface charges are formed by dimeric 12-*s*-12 surfactants with $6 \leq s \leq 12$.

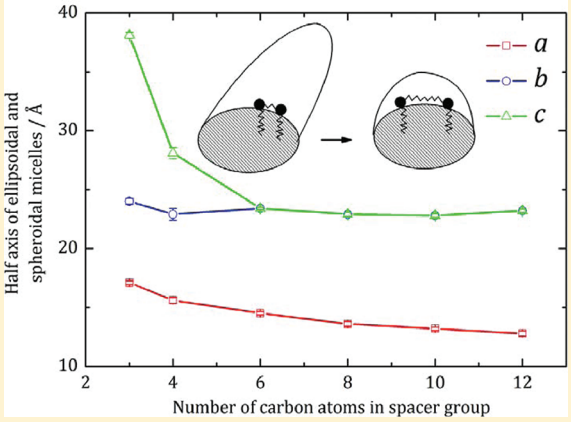

INTRODUCTION

A dimeric or Gemini surfactant is a type of surfactant where two conventional single-chain surfactants are chemically attached to one another via a spacer unit.[1] A common type of cationic dimeric surfactant is the bis-quaternary surfactant alkanediyl-α,ω-bis(dimethyl ammonium bromide) ($C_mH_{2m+1}N(CH_3)_2(CH_2)_sN(CH_3)_2C_mH_{2m+1}Br_2$) or, in shorter form, *m*-*s*-*m* surfactant, where *m* denotes the number of carbon atoms in the aliphatic hydrocarbon chain of a surfactant tail and *s* is the number of methylene units in the spacer group.[2−5] A typical feature of surfactant molecules is that they self-assemble above the critical micelle concentration (cmc) to form micelles or bilayers. The entropy of mixing a dimeric surfactant and solvent is from an entropic point of view less favorable than mixing twice the amount of a single-chain surfactant, i.e., the same number of chains, and as a consequence, dimeric surfactants have been found to feature much lower cmc values as compared to the corresponding unimeric surfactant.

The growth rate, in terms of measurements of the aggregation number N as a function of surfactant concentration c_{surf}, for micelles formed by the dimeric surfactant series 12-*s*-12 has previously been investigated by Danino et al.[5] with time-resolved fluorescence quenching (TRFQ). It was found that two of the dimeric surfactants, 12-3-12 and 12-4-12, display a considerable growth with respect to surfactant concentration, i.e., d ln N/d ln $c_{surf} \approx 1$ or slightly below [cf. Figure 3 in ref 5]. More recently, a similar substantial growth rate for micelles formed by 12-2-12 and 12-3-12 dimeric surfactants was observed by In et al.[6] using small-angle neutron scattering (SANS). A micelle growth behavior in accordance with d ln N/d ln $c_{surf} = 1$ is expected for rodlike micelles that grow exclusively in the length direction. The reason for this behavior is that the local curvature of a rodlike micelle does not change during the growth process and each added surfactant molecule is incorporated in the central part (as opposed to the end-caps) of the rod. In accordance, the following relation for the average

Received: March 21, 2012
Revised: May 24, 2012
Published: May 24, 2012

   dx.doi.org/10.1021/la301190d | *Langmuir* 2012, 28, 9311−9321

aggregation number $\langle N \rangle = e^{\alpha}\phi_{mic}$ has been derived for rodlike micelles that grow exclusively in length, where α is the curvature free energy of the micellar end-caps and ϕ_{mic} is the volume fraction of aggregated surfactants.[7−9] The above relation for the growth behavior of elongated micelles was derived using the proper expression, with volume fraction rather than mole fraction, for the entropy of mixing objects with different sizes (micelles and solvent molecules in the present case).[10,11] We may note that using mole fraction in the aforementioned derivation gives a flaw expression for the growth relation, according to which $\langle N \rangle \propto \phi_{mic}^{1/2}$, which may sometimes be seen in the literature. A growth relation with $\langle N \rangle \propto \phi_{mic}$ for elongated micelles is supported by several scattering and TRFQ measurements for ordinary surfactant micelles, for instance those presented for 12-3-12 and 12-4-12 in ref 5. Using volume fraction in the expression for the entropy of mixing also gives rise to a relative standard deviation $\sigma_N/\langle N \rangle = 1$ for the volume-weighted size distribution of long rodlike or wormlike micelles, which is in agreement with experimental observations using SANS.[12,13]

Most interestingly, the growth behavior of micelles formed by 12-*s*-12 surfactants with a spacer group corresponding to $s \geq 5$ is found to be completely different as compared to 12-3-12- and 12-4-12 surfactant micelles. In accordance, the growth rate of micelles formed by 12-5-12, 12-6-12, 12-8-12, and 12-10-12 is found to be very low, i.e., d ln N/d ln $c_{surf} < 0.1$ [cf. Figure 3 in ref 5].[5] The latter behavior is similar to what has been observed for the corresponding unimeric surfactant dodecyltrimethylammonium bromide (DTAB) for which N was found to be, within experimental errors, independent of c_{surf}.[14]

Values of the growth rate d ln N/d ln c_{surf} close to zero have traditionally been rationalized as a result of the micelles being shaped as spheres rather than elongated rods, since the local curvature of spherical micelles must change due to geometrical reasons as the micelles grow in size. For this reason, it was concluded in ref 5 that 12-5-12, 12-6-12, 12-8-12, and 12-10-12 form monodisperse spherical micelles. However, the growth behavior of strictly spherical micelles must be limited in the sense that the aggregation number must never exceed the value corresponding to a sphere with a radius equal to the fully stretched out surfactant tail.[15,16] As a result, one would expect that the growth rate of spherical micelles, at some point where the micelles start to grow in the length direction, abruptly increases to approach the value expected for rodlike micelles. This behavior could, however, not be observed in the TRFQ measurements reported in ref 5.

Moreover, micelles formed by 12-*s*-12 surfactants with $s \geq 5$, at high surfactant concentrations, were observed to be larger than micelles formed by 12-3-12 in very dilute solutions, although the growth rate of micelles formed by the latter surfactant was found to be much higher.[5] For instance, 12-10-12 has an aggregation number equal to about $N = 40$, corresponding to a radius $R = 22.3$ Å of a spherical micelle, at a surfactant concentration about $c = 200$ mM, whereas $N \leq 30$ for 12-3-12 ($R \leq 19.1$ Å) below about $c = 10$ mM. Obviously there is no unequivocal correlation between size and growth rate for micelles formed by dimeric surfactants with different spacer group lengths. Thus, it is indicated by the TRFQ measurements in ref 5 that the difference in growth rate observed for micelles formed by dimeric surfactants with different spacer lengths (12-3-12 and 12-4-12, on one hand, and 12-5-12, 12-6-12, 12-8-12, and 12-10-12, on the other hand) must have a fundamentally different explanation than the one offered by considering the micelles either as spheres or as elongated prolate spheroids/spherocylinders.

A similar behavior of different growth rates ranging from d ln N/d ln c_{surf} slightly above zero to unity has also been observed for pure micelles formed by $C_{12}H_{25}NH_n(CH_3)_{3-n}Cl$ surfactants with $0 \leq n \leq 3$.[17] The conspicuously different growth behaviors for micelles depending on the chemical structure of the constituent surfactant indicate some fundamental differences in the geometrical structure of the micelles. In the present article, we investigate the self-assembly of various dimeric 12-*s*-12 surfactants with SANS. Our specific aim is to correlate the micellar growth rate, as previously observed with TRFQ in ref 5, with the detailed geometrical shape of micelles formed by dimeric 12-s-12 surfactants with different lengths of the spacer group.

The detailed geometry of micelles formed by the unimeric surfactants sodium dodecylsulfate (SDS) and DTAB at different concentrations of added NaBr have previously been investigated with SANS.[12] Several models were considered and the agreement between each model and data were compared. In accordance, it was concluded that both SDS and DTAB micelles were shaped as oblate spheroids that may grow into triaxial general ellipsoids upon increasing the electrolyte concentration. Later on, general ellipsoidal micelles have been observed in several pure[18] as well as mixed surfactant systems[13,19−23] using SANS.

Micelles formed by anionic,[24−26] cationic,[6,27−32] and nonionic[33,34] dimeric surfactants have previously been investigated with SANS. In most cases the aggregation number of micelles is found to decrease as the length of the spacer group is increased. For instance, micelles formed by $C_{10}H_{21}N(CH_3)_2(CH_2)_sN(CH_3)_2C_{10}H_{21}$ (10-*s*-10) surfactants were investigated by Hirata et al.[27] and analyzed with a core−shell model for prolate spheroids. It was found that the aggregation number decreases as the spacer length increases from $s = 2$ to 6. Likewise, the growth rate was observed to significantly decrease in magnitude with increasing s, and the aggregation number of 10-6-10 surfactant micelles were found be virtually constant with respect to surfactant concentration.

Micelles formed by 16-*s*-16 surfactants have been investigated by Aswal et al.[28] In accordance, 16-3-16 surfactant micelles were found to form rather large disks (disk radius equal to 200 Å) whereas large rodlike micelles were observed to be formed by 16-4-16. The micelles were seen to further decrease in size as s was increased from 5 to 12, and the corresponding SANS data were analyzed with a model for prolate spheroids. Triaxial ellipsoidal or oblate spheroidal micelle models were never considered in refs 27 and 28. Later on, however, a cationic dimeric surfactant based on $[Ru(bipy)_3][Cl]_2$ complexes were found to form oblate spheroidal micelles.[30]

Out of the dimeric bis-quaternary surfactants investigated in the present work, 12-4-12 has previously been studied with SANS.[35] Only one sample at a surfactant concentration equal to 100 mM at 30 and 50 °C, respectively, was measured and the corresponding SANS data were analyzed with a prolate spheroidal model. In a more recent work, the growth behavior of 12-2-12 and 12-3-12 surfactant micelles were investigated by In et al.[6] The micelle aggregation numbers were determined from the peak position of the apparent structure factor, whereas the detailed geometry of the micelles was not considered in the data analysis.

Bilayer structures have been observed with SANS to be formed by a catanionic surfactant composed of one cationic dimeric surfactant and two anionic unimeric surfactants[36] as well as by a dimeric surfactant (12-2-12) in presence of large amounts of added salt (KBr).[37] It is also known, from cryo-transmission electron microscopy measurements, that bilayer structures such as vesicles may form by dimeric surfactants with a comparatively long spacer group, for instance 12-16-12 and 12-20-12.[5]

MATERIALS AND METHODS

Materials. The dimeric Gemini surfactants used in the present study are of the type $C_{12}H_{25}N(CH_3)_2(CH_2)_sN(CH_3)_2C_{12}H_{25}$ (12-*s*-12) with s = 3, 4, 6, 8, 10, and 12 and were a gift to the research group of Surface Chemistry, KTH Royal Institute of Technology from Prof. Verall, University of Saskatchewan, Canada. The surfactants have been purified by recrystallization so that no minimum in surface tension could be observed in the pre cmc region.[38] This means that the surfactant purity is expected to be close to 100%. Deuterium oxide (D_2O) with 99.9 atom % D was purchased from Aldrich Chemical Co. and used as solvent.

Sample Preparation. Stock solutions were prepared by simply mixing the surfactants with D_2O to yield an overall surfactant concentration 18 mM. The less concentrated samples were obtained by means of diluting the stock solutions with deuterium oxide to obtain a surfactant concentration equal to 9 and 4.5 mM. An isotropic micellar L_1 phase was seen to form in all of our samples. Each sample was equilibrated for at least 24 h at room temperature (about 23 °C) before measurements. Pure D_2O (without any H_2O or buffer) was chosen as solvent in all experiments in order to minimize the incoherent background from hydrogen and obtain a high scattering contrast.

Methods. Small-angle neutron scattering (SANS) experiments were carried out at the SANS-1 instrument at the Geesthach Neutron Facility GeNF at Helmholtz Zentrum Geesthacht: Centre for Materials and Coastal Research, Geesthacht, Germany. A range of magnitudes of the scattering vector q from 0.005 to 0.25 $Å^{-1}$ was covered by three combinations of sample-to-detector distances (0.7–9.7 m) at a neutron wavelength of 8.5 Å. The wavelength resolution was $\Delta\lambda/\lambda$ = 10% (full-width-at-half-maximum value).

The samples were kept in quartz cells (Hellma) with a path length of 2 mm. The raw spectra were corrected for background from the solvent, sample cell, and other sources by conventional procedures.[39] The two-dimensional isotropic scattering spectra were azimuthally averaged, converted to an absolute scale, and corrected for detector efficiency by dividing by the incoherent scattering spectra of pure water measured in a 1 mm cell.[40] The spectra from pure solvent (deuterium oxide) in a cuvette with identical path length were measured and subtracted from the spectra for each sample. The scattering intensity was finally normalized by dividing with the surfactant concentrations in g/mL, giving the unit [mL g^{-1} cm^{-1}] for the normalized scattering intensity $d\sigma_m/d\Omega \equiv (d\sigma/d\Omega)/c_{surf}$.[41]

Throughout the data analysis, corrections were made for instrumental smearing.[42,43] For each instrumental setting the ideal model scattering curves were smeared by the appropriate Gaussian resolution function when the model scattering intensity was compared with the measured one by means of least-squares methods.

The average excess scattering length density per unit mass of solute for the different surfactants in D_2O ($\Delta\rho_m$) was calculated using the appropriate molecular volume ($\hat{v}$) and molecular weight (M_{surf}) of the surfactant monomers [cf. Table 1].[44] The molecular volume of DTAB given in Table 1 has previously been determined by Corkill et al.[45] The corresponding volume for the spacer group of dimeric surfactants was calculated using partial molar volumes for alkyl chains dispersed in water.[46] However, the volume occupied by hydrocarbon groups immersed in water has been found to be considerably smaller than the corresponding molecular volume for hydrocarbons immersed in a hydrocarbon solvent.[44,46] The spacer groups of surfactants aggregated in micelles is located in proximity to the hydrocarbon/water interface and, as a result, our values of the molecular volumes given in Table 1 may be somewhat underestimated. In Table 1, we have also included previously determined critical micelle concentrations for the various dimeric surfactants[4] as well as for the unimeric surfactant DTAB[47].

Table 1. Molecular Weight (M_{surf}), Molecular Volume ($\hat{v}$), Excess Scattering Length Density ($\Delta\rho_m$), and Critical Micelle Concentration (cmc)[4,47] for Surfactants Investigated in the Present Paper

	M_{surf}/g mol^{-1}	$\hat{v}$/$Å^3$	$\Delta\rho_m$/cm g^{-1}	cmc/mM
DTAB	308.35	491.0	-6.37×10^{10}	15.4
12-3-12	628.7	973.6	-6.12×10^{10}	0.91
12-4-12	642.7	1000	-6.15×10^{10}	1.00
12-6-12	670.8	1053	-6.21×10^{10}	1.12
12-8-12	698.8	1106	-6.25×10^{10}	0.89
12-10-12	726.9	1158	-6.32×10^{10}	0.32
12-12-12	754.9	1211	-6.37×10^{10}	0.28

Data Analysis. The normalized scattering cross section as a function of scattering vector q for a sample of monodisperse nonspherical particles can be written as follows:

$$\frac{d\sigma_m(q)}{d\Omega} = \Delta\rho_m{}^2 M_w P(q)[1 + \beta(q)(S(q) - 1)] \quad (1)$$

where $\Delta\rho_m$ is the difference in scattering length per unit mass solute between particles with a homogeneous core and solvent, M_w is the molar mass of a particle, and $P(q) \equiv \langle F^2(q)\rangle_0$ is the orientational averaged form factor.[41] The structure factor $S(q)$ has been included using a so-called decoupling approximation, where $\beta(q) \equiv \langle F(q)_0{}^2\rangle / \langle F^2(q)\rangle_0$, valid for particles with small anisotropy.[48,49]

SANS data from samples with 12-3-12 and 12-4-12 were found to be best fitted using a model for triaxial general ellipsoids with half axis a, b, and c, where $a < b < c$. The orientational averaged form factor for triaxial ellipsoids equals

$$\langle F^2(q)\rangle_0 = \frac{2}{\pi}\int_0^{\pi/2}\int_0^{\pi/2} F^2(q, r(a, b, c, \phi, \theta)) \sin\phi \, d\phi \, d\theta \quad (2)$$

where $F(q, r) = 3[\sin(qr) - qr\cos(qr)]/(qr)^3$ and $r(a,b,c,\phi,\theta) = ((a^2 \sin^2\theta + b^2\cos^2\theta)\sin^2\phi + c^2\cos^2\phi)^{1/2}$.[50] Interactions have been taken into account by means of using a structure factor $S(q)$ including repulsive excluded volume interactions as well as electrostatic double-layer forces as derived by Hayter and Penfold[51] from the Ornstein–Zernike equation in the rescaled mean spherical approximation.[52]

The micelles formed by DTAB, 12-6-12, 12-8-12, 12-10-12, and 12-12-12 were found to be rather small and the corresponding SANS data were best fitted with a model for biaxial (oblate or prolate) spheroids, i.e.[53]

$$\langle F^2(q)\rangle_0 = \int_0^{\pi/2} F^2(q, r(a, b, \phi)) \sin\phi \, d\phi \quad (3)$$

where $r(a,b,\phi) = ((a^2 \sin^2\phi + b^2\cos^2\theta)^{1/2}$.

The parameters in the model were optimized by means of conventional least-squares analysis and their errors were calculated with conventional methods.[41,54] The quality of the fits were measured in terms of the reduced chi-squared parameter defined as

$$\chi^2 = \frac{1}{N - M}\sum_{i=1}^{N}\left(\frac{I_{exp}(q_i) - I_{mod}(q_i)}{\sigma_i}\right)^2 \quad (4)$$

where $I_{exp}(q_i)$ and $I_{mod}(q_i)$ are the experimental and model intensities, respectively, at a scattering vector modulus q_i. σ_i is the statistical uncertainties on the data points, N is the total number of data points, and M is the number of parameters optimized in the model fit. The statistical errors of the fitting parameters corresponds to a change in m^2, defined as $m^2 \equiv \chi^2(N - M)/N$, equal to 0.1.

dx.doi.org/10.1021/la301190d | Langmuir 2012, 28, 9311–9321

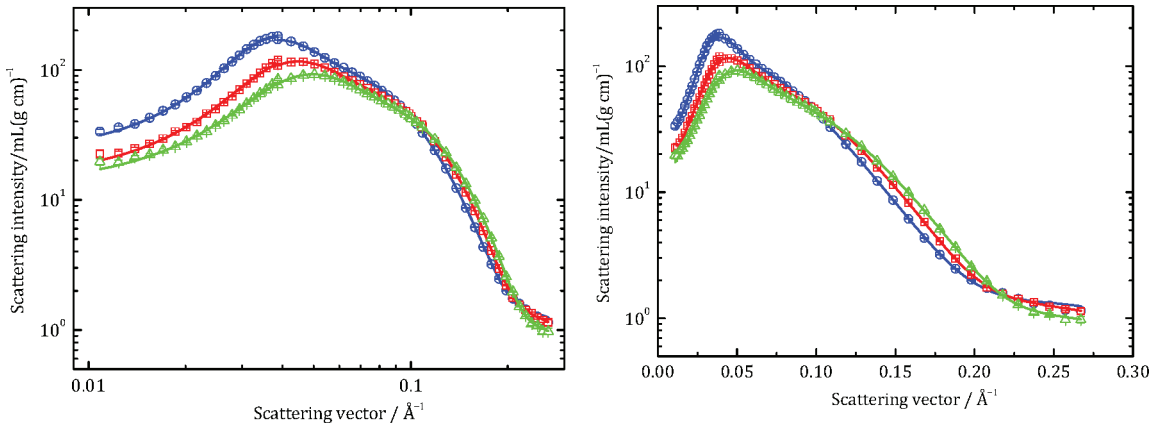

Figure 1. Normalized scattering cross section as a function of the scattering vector q for the dimeric surfactants 12-3-12 (circles), 12-4-12 (squares), and 12-6-12 (triangles) in deuterium oxide. The total surfactant concentration is [12-s-12] = 18 mM. Individual symbols represent SANS data obtained for different sample−detector distances. The solid lines represent the best available fit with a model for a general ellipsoid (circles and squares) or an oblate spheroid (triangles). The results of the fits are given in Table 2. The quality of the fits as measured by χ^2 are 7.4 (circles), 3.7 (squares), and 7.5 (triangles). Both graphs show identical data and model fits but on different scales of the x axis. The scattering behavior at high q values is emphasized by the graphs on a semilogarithmic scale shown to the right.

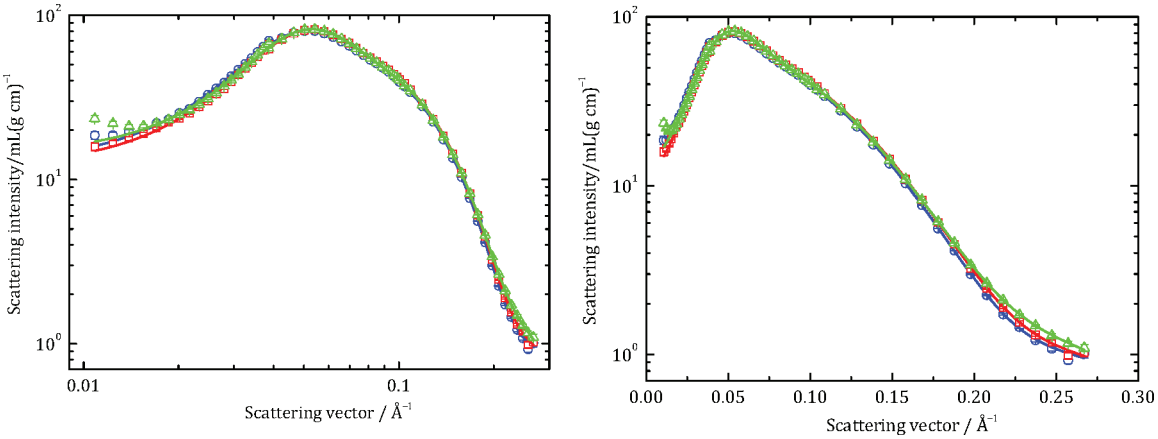

Figure 2. Normalized scattering cross section as a function of the scattering vector q for the dimeric surfactants 12-8-12 (circles), 12-10-12 (squares), and 12-12-12 (triangles) in deuterium oxide. The total surfactant concentration is [12-s-12] = 18 mM. Individual symbols represent SANS data obtained for different sample−detector distances. The solid lines represent the best available fit with a model for an oblate spheroid. The results of the fits are given in Table 2. The quality of the fits as measured by χ^2 are 8.5 (circles), 9.6 (squares), and 10.2 (triangles). Both graphs show identical data and model fits but on different scales of the x axis. The scattering behavior at high q values is emphasized by the graphs on a semilogarithmic scale shown to the right.

The number of fitting parameters, including the residual incoherent background scattering, is M = 6 or 7. The number of SANS data points is about N = 60. We have aimed at keeping our models as simple as possible and always been careful not to introduce any additional fitting parameters unless they give rise to a significant improvement of the quality of the model fits. The model fits could not be further improved using a core−shell model, and as a result, we have always employed a model for aggregates with a homogeneous and uniform scattering length density. A homogeneous scattering length density model is reasonable considering that both head groups and spacer unit of the dimeric surfactants have virtually identical scattering length densities as the hydrocarbon tails and that the largely hydrophobic spacer unit is expected to be attached in the vicinity of , or even partly dissolved into, the micelle core.

RESULTS AND DISCUSSION

Determination of Geometrical Shape of Micelles. SANS data together with model fits for different dimeric surfactants at a surfactant concentration equal to 18 mM are shown in Figure 1 (12-3-12, 12-4-12, and 12-6-12) and Figure 2 (12-8-12, 12-10-12, and 12-12-12), respectively, and the results from the model fitting analysis are given in Table 2.

We have recently investigated micelles formed by the unimeric surfactant DTAB, which have an identical C_{12} hydrocarbon chain as compared with the different dimeric surfactants investigated in the present work.[22] It was found that DTAB form oblate spheroidal micelles with half axes a = 14 Å and b = 24 Å (slightly better agreement with experimental data as compared to a model for prolate spheroids). The result agrees very well with what has previously been obtained for DTAB micelles at 40 °C, the micelles of which were observed to have an identical oblate spheroidal shape, with similar minor half axis but slightly smaller major half axis (b = 21 Å).[12] It is also well-known that DTAB micelles display a very small growth rate that resembles the case of dimeric 12-s-12 surfactants with $5 \leq s \leq 10$.[14]

Rather elongated tablet-shaped micelles are seen to be formed by 12-3-12, and the SANS data were best fitted with a model for triaxial general ellipsoids with half axes related to

dx.doi.org/10.1021/la301190d | Langmuir 2012, 28, 9311−9321

Table 2. Results from Least Square Model Fit Analysis of SANS Data[a]

	12-3-12	12-4-12	12-6-12	12-8-12	12-10-12	12-12-12
18 mM	a = 17.1	a = 15.6	a = 14.5	a = 13.6	a = 13.2	a = 12.8
	b = 24.0	b = 22.9	$b = c$ = 23.4	$b = c$ = 22.9	$b = c$ = 22.8	$b = c$ = 23.2
	c = 38.1	c = 28.1	N = 32	N = 27	N = 25	N = 24
	N = 67	N = 42	N^* = 26	N^* = 22	N^* = 20	N^* = 19
	N^* = 52	N^* = 34	α = 0.25	α = 0.26	α = 0.28	α = 0.31
	α = 0.22	α = 0.23	c_{mic} = 14 mM	c_{mic} = 14 mM	c_{mic} = 14 mM	c_{mic} = 13 mM
	c_{mic} = 15 mM	c_{mic} = 14 mM	c_{el} = 5 mM	c_{el} = 5 mM	c_{el} = 6 mM	c_{el} = 6 mM
	c_{el} = 6 mM	c_{el} = 5 mM				
9 mM	a = 16.8	a = 15.3	a = 14.2	a = 13.4	a = 13.4	a = 13.2
	b = 23.9	b = 22.6	$b = c$ = 22.7	$b = c$ = 22.0	$b = c$ = 21.7	$b = c$ = 22.1
	c = 32.8	c = 27.1	N = 29	N = 25	N = 23	N = 22
	N = 56	N = 39	N^* = 25	N^* = 21	N^* = 19	N^* = 18
	N^* = 46	N^* = 32	α = 0.26	α = 0.29	α = 0.34	α = 0.33
	α = 0.15	α = 0.22	c_{mic} = 7 mM	c_{mic} = 7 mM	c_{mic} = 7 mM	c_{mic} = 7 mM
	c_{mic} = 8 mM	c_{mic} = 7 mM	c_{el} = 3 mM	c_{el} = 3 mM	c_{el} = 4 mM	c_{el} = 3 mM
	c_{el} = 2 mM	c_{el} = 3 mM				
4.5 mM	a = 16.5	a = 15.7	a = 14.1	a = 12.7	a = 12.7	a = 12.5
	b = 23.2	b = 21.2	$b = c$ = 21.8	$b = c$ = 21.5	$b = c$ = 21.2	$b = c$ = 21.6
	c = 31.5	c = 26.8	N = 27	N = 22	N = 21	N = 20
	N = 52	N = 37	N^* = 25	N^* = 22	N^* = 18	N^* = 17
	N^* = 47	N^* = 31	α = 0.22	α = 0.27	α = 0.33	α = 0.35
	α = 0.13	α = 0.32	c_{mic} = 4 mM	c_{mic} = 3 mM	c_{mic} = 4 mM	c_{mic} = 4 mM
	c_{mic} = 4 mM	c_{mic} = 3 mM	c_{el} = 2 mM	c_{el} = 2 mM	c_{el} = 2 mM	c_{el} = 2 mM
	c_{el} = 1 mM	c_{el} = 6 mM				

[a]Samples with micelles were fitted with a model for general ellipsoids with half axes a, b, and c (in units of Ångström). N and N^* denote the aggregation numbers as determined from SANS data with two independent methods. α is the relative effective charge of the micelles, c_{mic} is the concentration of surfactant aggregated in micelles, and c_{el} is the electrolyte concentration.

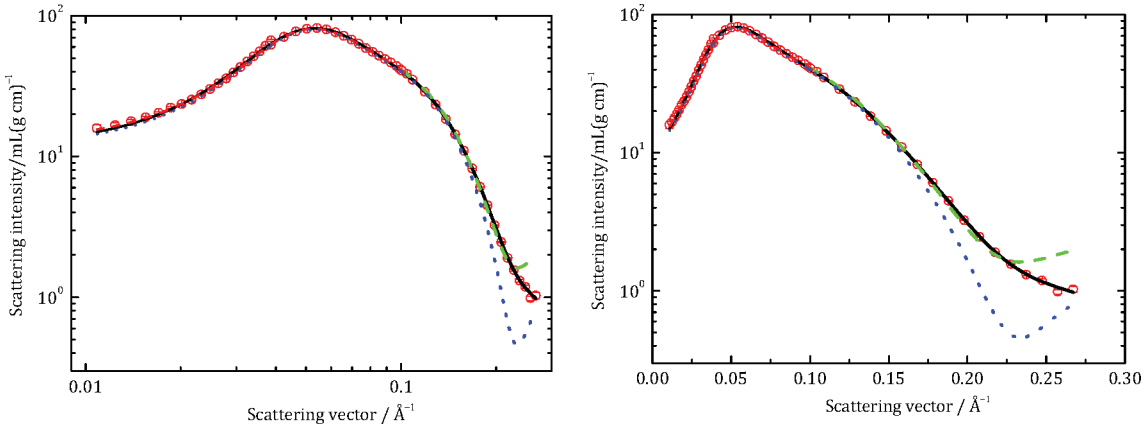

Figure 3. Normalized scattering cross section as a function of the scattering vector q for the dimeric surfactant 12-10-12 in D_2O. The total surfactant concentration is [12-10-12] = 18 mM. Individual symbols represent SANS data obtained for different sample−detector distances. The solid lines represent the best available fit with a model for oblate spheroids. The dashed line represents the best available fit with a model for monodisperse spheres. The dotted line represents the scattering curve for the monodisperse sphere model with a background scattering intensity set to the identical value as obtained from the model fit for oblate spheroids. The quality of the fits as measured by χ^2 are 9.6 (solid line) and 73.4 (dashed line). Both graphs show identical data and model fits but on different scales of the x axis. The scattering behavior at high q values is emphasized by the graphs on a semilogarithmic scale shown to the right.

thickness (a), width (b), and length (c), respectively, i.e., $a < b < c$. This model gives significantly better agreement with SANS data than, for instance, a core−shell prolate spheroidal model. The aggregation number of the micelles is found to increase substantially with increasing surfactant concentration, in agreement with what has previously been observed for the same surfactant with TRFQ.[5] Our SANS data analysis clearly shows that the micelles increase mainly in the length direction, i.e., the half axis related to length increases from c = 31.5 Å at 4.5 mM to c = 38.1 Å at 18 mM, whereas the half axes related to thickness and width, respectively, are found to be rather constant with respect to c_{surf}. The micelles formed by the 12-4-12 surfactant are significantly smaller in size than 12-3-12 micelles, but still show a triaxial ellipsoidal shape [cf. Figure 1 and Table 2].

It is well-known that micelles with a substantial growth rate with respect to surfactant concentration must be considerably polydisperse [cf. eq 5 below]. However, due to the strong double-layer interactions between charged surfactant micelles in absence of added salt, we are not able to incorporate

dx.doi.org/10.1021/la301190d | Langmuir 2012, 28, 9311−9321

polydispersity effects into our model fitting analysis of elongated ellipsoidal micelles.

Micelles formed by dimeric surfactants with a longer spacer unit, i.e., 12-6-12, 12-8-12, 12-10-12, and 12-12-12, are found to be considerably smaller than 12-3-12 and 12-4-12 surfactant micelles and were best fitted with a model for biaxial spheroids. The micelles appear to be somewhat smaller than DTAB micelles, and since we lack data in the regime $q > 0.25$ Å^{-1}, it is difficult to distinguish between oblate and prolate spheroidal shapes by means of comparing the quality of the model fits. It is found that oblate spheroidal shape gives a slightly better agreement between model and data at high surfactant concentrations, i.e., c_{surf} = 18 mM, whereas we could not distinguish between the two models for samples with lower values of c_{surf}, the data of which have somewhat larger statistical errors. However, it is well-known that elongated micelles, such as prolate spheroids, are expected to grow significantly in length with an increasing surfactant concentration in a similar manner as was seen for 12-3-12 and 12-4-12 micelles, i.e. with d ln N/d ln $c_{surf} \approx 1$.[7,9,55] Hence, the formation of prolate or spherocylindrical micelles by 12-6-12, 12-8-12, and 12-10-12 is inconsistent with the growth behavior as observed in TRFQ measurements reported in Reference 5. The moderate growth rate of surfactant micelles formed by 12-s-12 with $6 \leq s \leq 12$ is also supported by the aggregation numbers shown in Table 2 as obtained from our present SANS investigation at different surfactant concentrations.

Nonelongated oblate or disklike micelles, on the other hand, are bound to change the local curvature upon increasing in size and, similar to the behavior of spherical micelles, they are expected to grow only slightly with increasing values of c_{surf}. Unlike spherical micelles, however, oblate micelles may grow indefinitely without any need to change geometry during the growth process. Both these features agree very well with the growth behaviors of 12-6-12, 12-8-12, and 12-10-12 dimeric surfactant micelles as reported in ref 5.

A typical example for the best available fit with a model for strictly spherical micelles (for the surfactant 12−10−12) is shown in Figure 3. It is seen that it deviates largely from the experimental SANS data above about q = 0.2 Å^{-1}, although the fitting parameter due to the residual background scattering intensity is optimized so as to minimize the reduced chi-square, χ^2. In order to visualize the latter effect, we have also included the scattering behavior of a model for monodisperse spheres, but with the background scattering set to the same value as obtained from the fitting procedure with a model for oblate spheroids. Moreover, the agreement between data and model for monodisperse spheres could not be significantly improved including a core−shell structure in the model, using realistic values for the appropriate scattering length densities, i.e. with a higher contrast between core and solvent than between shell and solvent.

It is known that the agreement between model fit and data in the high-q range may be significantly improved if the spherical micelles are assumed to be considerably polydisperse.[12,56] In order to obtain an acceptably good agreement between model and data shown in Figure 3, a polydispersity as high as $\sigma_R/\langle R\rangle \approx 0.2$ is required, where σ_R is the standard deviation with respect to sphere radius R and $\langle R\rangle$ is the corresponding average quantity. Assuming a Gaussian distribution, $\sigma_R/\langle R\rangle = 0.2$ means that 5% of the largest spheres in the size distribution must have a radius larger than about 23−24 Å. This value is much larger than the length of a fully stretched out C_{12} aliphatic chain (= 16.7 Å).[57] Head groups are expected to contribute with only a few extra Ångtröms to this value. In other words, assuming a strictly spherical shape of the micelles implies that the surfactant molecules are not able to reach the center of the largest micelles in the size distribution.

Moreover, it was concluded from TRFQ measurements that micelles formed by 12-6-12, 12-8-12, and 12-10-12, which all display a very low growth rate, are considerably monodisperse.[5] This observation agrees very well with the following equation:

$$\left(\frac{\sigma_N}{\langle N\rangle}\right)^2 = \frac{\mathrm{d}\ln\langle N\rangle}{\mathrm{d}\ln c_{surf}} \tag{5}$$

which relates the growth rate of micelles with polydispersity in terms of the relative standard deviation.[58,59] As a result of the geometrical relation $N\hat{v} = 4\pi R^3/3$, a relative standard deviation $\sigma_R/\langle R\rangle = 0.2$, based on the distribution of radii, corresponds to $\sigma_N/\langle N\rangle \approx 0.5$ for the distribution with respect to aggregation number N. This means that the SANS data for a model of polydisperse spheres corresponds to a growth rate d ln N/d ln $c_{surf} \approx 0.25$. This value is inconsistent with the TRFQ measurements reported in ref 5, according to which d ln N/d ln $c_{surf} < 0.1$ for micelles formed by 12-6-12, 12-8-12, and 12-10-12.

As a consequence, the geometries of prolate spheroid, cylinder and polydisperse sphere are all inconsistent with the growth behavior of micelles formed by 12-6-12, 12-8-12, and 12-10-12 as observed in previous TRFQ measurements[5] (and supported by our presently determined micelle aggregation numbers at different surfactant concentrations). The presence of monodisperse spherical micelles is consistent with TRFQ measurements, but inconsistent with our present SANS investigation [cf. Figure 3]. Hence, we are able to conclude that the oblate spheroid is the only shape of dimeric 12-6-12, 12-8-12, and 12-10-12 surfactant micelles that is consistent with both TRFQ and SANS. 12-12-12 was not investigated with TRFQ in ref 5, but appears to behave similarly as 12-6-12, 12-8-12, and 12-10-12 in our present SANS investigation.

The different half axes of ellipsoidal and spheroidal micelles, as obtained from our SANS data analysis, as functions of the length of the spacer group, are shown in Figure 4 for micelles formed at a fixed surfactant concentration c_{surf} = 18 mM. It is seen that the half axis related to thickness (a) decreases monotonously with increasing s. The half axis related to the width (b) of the micelles is found to be rather constant with respect to s, whereas the half axis related to the length (c) decreases considerably as s is increased from 3 to 6 to reach a rather constant value in the range $6 \leq s \leq 12$. Dimeric surfactants with s = 6, 8, 10, and 12 are found to form oblate spheroidal micelles with an almost identical major half axis (b), but with a half axis related to thickness (a) that decreases with increasing spacer length.

In Table 2 we have also included three fitting parameters related to the intermicelle interactions as taken into account by the Hayter−Penfold model[51] for the structure factor $S(q)$, i.e., concentration of surfactant aggregated in micelles (c_{mic}), electrolyte concentration (c_{el}), and effective charge of the micelles (z_{eff}). The latter quantity is expressed in terms of the ratio $\alpha \equiv z_{eff}/z_{id}$, where z_{id} is the charge of a fully dissociated macroionic micelle and is found to be in the range α = 0.13−0.35. The micelle and electrolyte concentrations are found to be in reasonable orders of magnitude considering that c_{el} is

dx.doi.org/10.1021/la301190d | Langmuir 2012, 28, 9311−9321

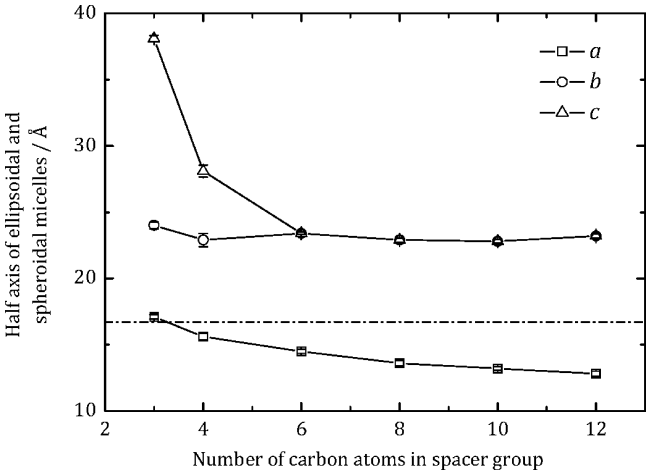

Figure 4. Half axes related to the thickness a (circles), width b (squares), and length c (triangles), as obtained from the least-squares model fitting analysis of SANS data, plotted against the number of methylene units in the spacer group (s) in 12-s-12 dimeric surfactants. The surfactant concentration is [12-s-12] = 18 mM. The dash-dotted line represents the length of a fully stretched out C_{12} aliphatic chain and indicate the maximum available radius for a strictly spherical micellar core.

expected to be close to cmc and $c_{mic} \approx$ [surfactant] − cmc in pure surfactants systems.[55,60]

The quality of our model fits is generally very good. Some deviations between model and data are nevertheless seen in Figures 1 and 2 at low q values. These discrepancies are probably due to various approximations in the derivation of the Hayter-Penfold structure factor. For instance, $S(q)$ is derived from the mean spherical approximation (MSA) extension of the Debye−Hückel theory, which assumes strictly spherical hard spheres with an electrostatic potential that is much lower than what corresponds to the surface charge density of the micelles investigated in the present work.[51]

Determination of Micellar Aggregation Numbers. The aggregation numbers for micelles formed by the various Gemini surfactants investigated in the present paper have been calculated in two different independent ways, and both corresponding values (N and N^*) are tabulated in Table 2. N was calculated from the half axes as obtained from the model fitting analysis, together with the geometrical relation $N\hat{v} = 4\pi abc/3$. N^* was calculated from the normalized absolute scale scattering intensity in the limit $\lim_{q\to 0} d\sigma/d\Omega$ by means of dividing with the dimeric surfactant molecular weight. In the latter method, we have taken into account the fact that a certain amount of surfactant (≈ cmc as given in Table 1) is not incorporated in the micelles. It is seen that N^* is systematically somewhat lower than N, indicating that the values of $\hat{v}$ shown in Table 1 are somewhat underestimated. The difficulties to determine $\hat{v}$ and N due to uncertainties in packing conditions of surfactant and solvent molecules are well-known.[44] As previously mentioned, when calculating $\hat{v}$ we have assumed that the spacer unit belongs to the headgroup and is surrounded by water molecules. Taking into account that parts of the spacer group is neighboring the hydrocarbon region of the micellar cores, one would expect somewhat higher values of $\hat{v}$ and aggregation numbers, as calculated with the two methods, closer to one another.

Our aggregation numbers for micelles formed by 12-6-12, 12-8-12, and 12-10-12 agree very well with what has previously been determined with TRFQ. For instance, the aggregation numbers are found to increase significantly with increasing surfactant concentration for 12-13-12 and 12-4-12 but only slightly for 12-6-12, 12-8-12, 12-10-12, and 12-12-12, indicating a very low polydispersity of micelles formed by the latter set of molecules. However, our values for 12-3-12 and 12-4-12 appear to be somewhat larger than those determined with TRFQ,[5] and the difference between N and N^* also appears to be larger for these two surfactants. For instance, the following values were obtained for the 12-3-12 surfactant,[5] N_{TRFQ} = 32 at 5 mM, 41 (10 mM), and 47 (20 mM) as compared to our results N = 52 and N^* = 47 (4.5 mM), N = 56 and N^* = 46 (9 mM), and N = 67 and N^* = 52 (18 mM). The discrepancy between the different methods for 12-3-12 and 12-4-12 is probably due to the considerably large polydispersity of the elongated micelles formed by the two surfactants and the fact that the average value of the distribution may be defined in some different ways. N^* refers to the weight or volume-averaged aggregation number. It is more difficult, however, to interpret N, since the micelles were assumed to be monodisperse in the model fitting data analysis (see above). We may also note that our measurements have been carried out with deuterium oxide as solvent whereas the TRFQ measurements were carried out in H_2O.

Our result for the aggregation number for 12-4-12 surfactant micelles N = 42 (N^* = 34) at 18 mM may be compared to the values N = 80 and 60 as obtained with SANS for the same surfactant at 100 mM and the two different temperatures 30 and 50 °C, respectively, using a prolate ellipsoidal model.[35] Likewise, our aggregation numbers for 12-3-12 at 18 mM (N = 67) agree very well with what was obtained by In et al.[6] at approximately equal surfactant volume fraction ($\phi \approx 0.01$). Notably, the aggregation number for 12-2-12 surfactant micelles was found by the same authors to exceed about N = 500 for concentrations $\phi > 0.01$.[6]

Dependence of Aggregation Number on Surfactant Spacer Length. In Figure 5 we have plotted the number of aggregated chains (= 2N for dimeric surfactants) relative to the

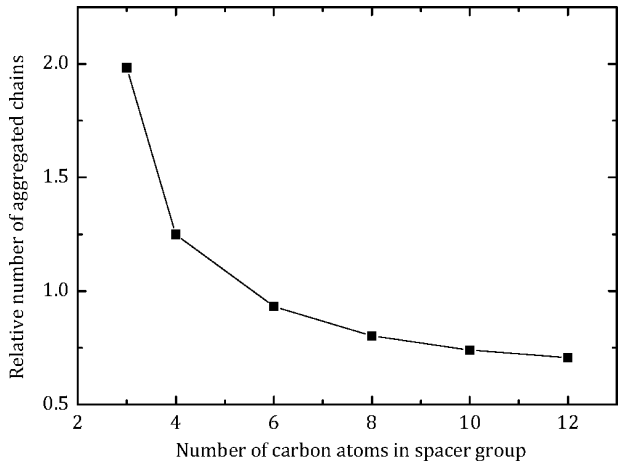

Figure 5. Number of aggregated alkyl chains in dimeric 12-s-12 surfactant micelles relative to the corresponding quantity for DTAB micelles ($2N/N_{DTAB}$), as obtained from the SANS data analysis, plotted against the number of methylene units in the spacer group (s) for samples with [12-s-12] = 18 mM. The aggregation number for the corresponding unimeric surfactant DTAB equals N_{DTAB} = 68 (at 30 mM).

dx.doi.org/10.1021/la301190d | Langmuir 2012, 28, 9311−9321

corresponding quantity for the unimeric surfactant DTAB, i.e., $2N/N_{DTAB}$, as a function of the number of methylene groups in the spacer group (s). It is seen that the number of aggregated chains for 12-3-12 and 12-4-12 micelles is appreciably larger as compared to DTAB micelles ($2N/N_{DTAB} > 1$). The aggregation number is found to monotonously decrease as the spacer length is increased from $s = 3$ to 12 and micelles formed by 12-6-12, 12-8-12, 12-10-12, and 12-12-12 have a lower number of self-assembled chains as compared to DTAB micelles ($2N/N_{DTAB} < 1$). $N_{DTAB} = 68$ at 30 mM has previously been determined with SANS.[22] Notably, DTAB has a comparably high cmc (~15 mM),[47] which means that the concentration of surfactant aggregated in micelles at [DTAB] = 30 mM is comparable to the corresponding quantity for our investigated Gemini surfactants at [12-s-12] = 18 mM.

The interfacial area per surfactant charge (a_{ch}) in the micelles has been calculated from the geometrical dimensions and aggregation numbers as obtained from our SANS data analysis. Details of the calculations are given in Supporting Information. The resulting values for micelles at surfactant concentrations equal to 18 mM are given in Table 3. For the sake of comparison, we have also included the corresponding value for the unimeric surfactant DTAB. There is an evident trend of increasing a_{ch} with increasing length of the spacer group as the two charges in a single molecule become increasingly more separated from one another. The trend agrees very well with previous observations of the area per surfactant for the same 12-s-12 surfactants as deduced from surface tension measurements.[4] In reference 4 it was also seen that the area per surfactant in the micelles reaches a maximum for a spacer length corresponding to about $s = 12$ and proceeds to decrease as s is further increased to 14 and 16. Hence, we may conclude that the intramolecular separation of charges appears to effectively give rise to repulsion between surfactant head groups in order to distribute the surface charges more uniformly over the micelle interface. As a result, surfactants with a short spacer group tend to form micelles with a high surface charge density implying that the surfactant head groups are more densely packed in the micelles. The surface charge and headgroup packing densities are found to decrease in magnitude, as the intramolecular charges become more separated with an increasing length of the spacer group. As a result, the micelles are seen to monotonously decrease in size with increasing s in Figure 5. Moreover, in Figure 4 it is seen that a_{ch} increases with increasing s mainly as a result of a decreasing half axis related to thickness (a), as the surfactant tails on average become more tilted with respect to the micelle interface.

Table 3. Interfacial Area Per Charge (a_{ch}), the Average Distance between Surface Charges at the Micelle Interface (d_{ch}), and the Distance between Two Intramolecular Charges for Different Dimeric Surfactants at [12-s-12] = 18 mM and DTAB at 30 mM

s	a_{ch}/Å^2	d_{ch}/Å	d_s/Å
DTAB	67.4	8.8	
3	63.6	8.6	5.1
4	73.1	9.2	6.3
6	71.7	9.1	8.9
8	79.2	9.6	11.4
10	83.7	9.8	13.9
12	88.4	10.1	16.4

Dependence of Micellar Geometrical Shape on Surfactant Spacer Length. We have previously analyzed the spatial dimensions of general triaxial tablet-shaped micelles in terms of the three bending elasticity constants spontaneous curvature (H_0), bending rigidity (k_c) and saddle-splay constant ($\bar{k}_c$) as defined in the so-called Helfrich expression.[22,23,61] For comparatively large tablet-shaped micelles (triaxial ellipsoids), it was possible to quantitatively estimate the three bending elasticity constants in order to rationalize the growth behavior of generally shaped micelles. The micelles formed by different dimeric surfactants studied in the present paper are, however, too small to allow for a quantification of k_cH_0, k_c, and $\bar{k}_c$. Nevertheless, the influence of the various bending elasticity constants on the geometrical shape and size of surfactant micelles may be qualitatively deduced from our previous analysis, which may be summarized as follows:[22,55,62] (i) The spontaneous curvature (or rather k_cH_0) is related to the magnitude of the curvature of the micelles and is found to mainly influence the width of micelles in such a way that the width (or half axis b) decreases with increasing values of k_cH_0. (ii) The bending rigidity (k_c) mainly influences the length of micelles so that the micelles become increasingly more elongated as k_c is decreased. k_c is also directly related to the growth rate and polydispersity of the micelles, i.e., k_c is expected to be comparatively large for micelles with a low growth rate and polydispersity and, as k_c decreases below about kT, the micelles are predicted to become substantially polydisperse with a growth rate approaching d ln N/d ln c_{surf} = 1. Notably, the bending rigidity must be a positive quantity for stable self-assembled interfacial aggregates, i.e., micelles or bilayers, to form and k_c is expected to increase in magnitude with increasing amphiphilic character of the surfactant molecule.[55,63] (iii) As a consequence of the Gauss-Bonnet theorem, the saddle-splay constant has an indirect influence on the micelle size in that way N increases with $\bar{k}_c$. (iv) Micelles are expected to form as $H_0 > 1/4\xi$, where ξ is the thickness of the self-assembled interface, whereas bilayers are expected to predominate as $H_0 < 1/4\xi$.

From the aforementioned criteria, it follows that the unimeric surfactant DTAB, which form oblate spheroidal micelles that only grow slightly with increasing surfactant concentration, must have a comparatively large bending rigidity. As two unimeric surfactants are linked with a propylene spacer unit to form 12-3-12, rather elongated general ellipsoidal micelles with a much higher growth rate form implying that k_c has become substantially reduced. The micelles become less elongated as the number of carbon atoms in the spacer unit increases from $s = 3$ to 12, which means that k_c becomes substantially raised as s is increased to reach a value similar to that of DTAB. The width of the micelles, on the other hand, is approximately constant with respect to s, which means that k_cH_0 is virtually uninfluenced by the length of the spacer group in the range $3 \leq s \leq 12$. Notably, our present conclusion that the experimentally observed N vs s dependence for dimeric surfactants is mainly caused by changes in bending rigidity differs from the explanation proposed in ref 3. In the latter work, it was suggested that the aggregation numbers of 12-2-12, 12-3-12, and 12-4-12 micelles decreases with an increasing length of the spacer group mainly as a result of an increasing spontaneous curvature.

dx.doi.org/10.1021/la301190d | Langmuir 2012, 28, 9311−9321

In Table 3 we have also included the average distance between two charges in the micelle (d_{ch}) as calculated assuming 2-dimensional hexagonal packing of the charged groups at the micellar interface. More details are given in the Supporting Information. This distance may be compared to the distance between two charges within a single dimeric surfactant (d_s) as estimated from the length of the spacer group. We have employed the following relation $d_s = 1.265(s + 1)$, based on the length of a fully stretched $-(CH_2)_s-$ chain, in order to calculate the latter quantity. It is seen that $d_s < d_{ch}$ for the two dimeric surfactants 12-3-12 and 12-4-12, respectively, which means that the surface charges must be significantly nonuniformly distributed over the interface of a micelle formed by a surfactant with such a short spacer group. A nonuniform distribution of surface charges is expected to give rise to low bending rigidities and micelles with a geometrically heterogeneous shape, i.e., a substantial difference in curvature between different geometrical parts of the micelle. For instance, the elongated micelle has a comparatively high proportion of rims, the geometry of which have a higher curvature as compared to other geometrical parts of the micelle. For the particular case of elongated ellipsoidal micelles formed by 12-3-12 and 12-4-12 surfactants, the two charges on a single molecule are located comparatively close to one another and tend to have a preference to be situated at the more curved rim parts of the oblong micelles. As the length of the spacer group is increased to $s = 6$, $d_s \approx d_{ch}$ and the surface charges may become more uniformly distributed over the micelle interface, giving rise to comparatively high bending rigidities. As a result, oblate spheroidal micelles that are less geometrically heterogeneous as compared to elongated micelles are observed to form by the dimeric 12-6-12 surfactant. As s is further increased, the spacer group becomes more flexible and the two alkyl chains in the dimeric surfactant molecule increasingly more independent of one another. The position of the surface charges become less restricted and may still remain more uniformly distributed over the micellar interface. As a result, the micelles are seen to keep their oblate spheroidal shape, whereas the half axis related to thickness of the micelles decreases as the distance between the two intramolecular charges increases and the surfactant head groups become less densely packed.

The distribution of distances between charges on interfaces of micelles formed by Gemini surfactants was already considered by Danino et al.[5] Similar to our present arguments, they concluded that charges on micelles formed by Gemini surfactants with a short spacer are nonuniformly distributed in a bimodal distribution, whereas a transition to a single-mode charge distribution occurs at a spacer length corresponding to about $s = 6-7$.

CONCLUSIONS

The geometrical structure of micelles formed by bis-quaternary dimeric Gemini surfactants 12-s-12, with $s = 3$, 4, 6, 8, 10, and 12, have been investigated with SANS. Micelles formed by 12-3-13 and 12-4-12 have previously been found to display a high growth rate, and according to our present investigation, the corresponding SANS data best agree with a model for oblong general ellipsoids with half axes a, b, and c. The micelles are found to monotonously decrease in length as the size of the spacer group is increased from $s = 3$ to 6, and the data for micelles formed by dimeric surfactants with $6 \leq s \leq 12$ agrees the best with a model for biaxial (oblate or prolate) spheroids, whereas a model for monodisperse spheres is always inconsistent with our SANS data.

In order to distinguish oblate from prolate spheroidal shape for micelles formed by 12-6-12, 12-8-12, 12-10-12, and 12-12-12, we have compared and correlated our SANS measurements with the growth behavior of micelles with respect to surfactant concentration as previously observed with time-resolved fluorescence quenching (TRFQ).[5] In accordance, the growth rate of micelles formed by 12-s-12 surfactants with $5 \leq s \leq 10$ was found to be close to zero in ref 5. Hence, out of the considered geometrical structures (oblate spheroids, prolate spheroids, monodisperse spheres, and polydisperse spheres), only the shape of oblate spheroids is consistent with both SANS and TRFQ. In other words, our results demonstrate that the micelles can be shaped as neither monodisperse spheres (inconsistent with our present SANS data), as previously suggested from TRFQ measurements, nor as prolate spheroids (inconsistent with micellar growth behavior), as usually assumed in earlier SANS data analyses of micelles formed by Gemini surfactants. As a result, we are able to reinterpret the structural behavior as previously suggested from TRFQ measurements and conclude that micelles formed by the surfactant series 12-s-12 decrease in size from substantially elongated tablet-shaped micelles ($s = 3$ and 4) to oblate spheroidal micelles as the length of the spacer groups increases beyond $s = 6$. The oblate micelles formed by dimeric 12-s-12 surfactants with $6 \leq s \leq 12$ are found to be structurally similar to micelles formed by the corresponding unimeric surfactant DTAB.

From analysis of our experimental results in terms of bending elasticity properties, based on the general micelle model, we are able to conclude that the dimeric surfactant micelles decrease in size from elongated tablets to more compact oblates mainly as a result of increasing values of the bending rigidity with an increasing spacer group length. The spontaneous curvature (or rather k_cH_0), on the other hand, is rather uninfluenced by the length of the spacer group. Simple geometrical considerations reveals that the intramolecular distance between two charges for the surfactants 12-3-12 and 12-4-12 is significantly smaller than the average distance between surface charges in a micelle. Hence, we argue that the surface charges in micelles formed by 12-3-12 and 12-4-12 must be substantially nonuniformly distributed, thus favoring the formation of geometrically heterogeneous oblong micelles, with a higher surface charge density in the more curved end-caps. As the spacer length equals $s = 6$, the intramolecular distance between two surfactant charges reaches a value approximately equal to the average distance between charges in the micelle, and as a consequence, the micelles tend to become shaped as oblate spheroids with the charges more uniformly distributed over the micelle interface.

ASSOCIATED CONTENT

Supporting Information

Additional experimental details. This material is available free of charge via the Internet at http://pubs.acs.org.

AUTHOR INFORMATION

Corresponding Author

*Tel: +46 8 790 99 21. Fax: +46 8 20 82 84. E-mail: magnusbe@kth.se.

Notes

The authors declare no competing financial interest.

■ ACKNOWLEDGMENTS

This work was supported by the Swedish Research Council. The SANS measurements were supported by the European Commission (Grant Agreement No. 226507-NMI3).

■ REFERENCES

(1) Zana, R.; Xia, J. *Gemini Surfactants: Synthesis, Interfacial and Solution-Phase Behavior and Applications*; Dekker: New York, 2004.
(2) Zana, R.; Benrraou, M.; Rueff, R. Alkanediyl-bis-(dimethylalky1ammonium bromide) surfactants. 1. Effect of the spacer chain length on the critical micelle concentration and micelle ionization degree. *Langmuir* **1991**, *7*, 1072−1075.
(3) Zana, R.; Talmon, Y. Dependence of aggregate morphology on structure of dimeric surfactants. *Nature* **1993**, *362*, 228−230.
(4) Alami, E.; Beinert, G.; Marie, P.; Zana, R. Alkanediyl-bis-(diemtylammonium bromide) surfactants (dimeric surfactants). 3. Behaviour at the air-water interface. *Langmuir* **1993**, *9*, 1465−1467.
(5) Danino, D.; Talmon, Y.; Zana, R. Alkanediyl-bis-(diemtylammonium bromide) surfactants (dimeric surfactants). 5. Aggregation and microstructure in aqueous solutions. *Langmuir* **1995**, *11*, 1448−1456.
(6) In, M.; Bendjeriou, B.; Noirez, L.; Grillo, I. Growth and branching of charged wormlike micelles as revealed by dilution laws. *Langmuir* **2010**, *26*, 10411−10414.
(7) Eriksson, J. C.; Ljunggren, S. The mechanics and thermodynamics of rod-shaped micelles. *J. Chem. Soc., Faraday Trans. 2* **1985**, *81*, 1209−1242.
(8) Eriksson, J. C.; Ljunggren, S. Model calculations on the transitions between surfactant aggregates of different shapes. *Langmuir* **1990**, *6*, 895−904.
(9) Bergström, M. Thermodynamics of micelles and vesicles. In *Handbook of Surfaces and Interfaces of Materials*; Nalwa, H. S., Ed.; Academic Press: San Diego, 2001; Vol. 5: Biomolecules, Biointerfaces and Applications, pp 233−264.
(10) Guggenheim, E. A. *Mixtures*; Clarendon Press: Oxford, 1952.
(11) Flory, P. J. Thermodynamics of polymer solutions. *Faraday Discuss.* **1974**, *57*, 7−29.
(12) Bergström, M.; Pedersen, J. S. Structure of pure SDS and DTAB micelles in brine determined by small-angle neutron scattering (SANS). *Phys. Chem. Chem. Phys.* **1999**, *1*, 4437−4446.
(13) Bergström, M.; Pedersen, J. S. A small-angle neutron scattering (SANS) study of tablet-shaped and ribbonlike micelles formed from mixtures of an anionic and a cationic surfactant. *J. Phys. Chem. B* **1999**, *103*, 8502−8513.
(14) Lianos, P.; Lang, J.; Zana, R. Fluorescence probe study of the effect of concentration on the state of aggregation of dodecylalkyldimethylammonium bromides and dialkyldimethylammonium chlorides in aqueous solution. *J. Colloid Interface Sci.* **1983**, *91*, 276−279.
(15) Tartar, H. V. A theory of the structure of the micelles of normal paraffin chain salts in aqueous solution. *J. Phys. Chem.* **1955**, *59*, 1195−1199.
(16) Tanford, C. Micelle shape and size. *J. Phys. Chem.* **1972**, *76*, 3020−3024.
(17) Malliaris, A.; Lang, J.; Zana, R. Dynamics of micellar solutions of ionic surfactants by fluorescence probing. *J. Phys. Chem.* **1986**, *90*, 655−660.
(18) Kadi, M.; Hansson, P.; Almgren, M.; Bergström, M.; Garamus, V. M. Mixed micelles of fluorocarbon and hydrocarbon surfactants. A small angle neutron scattering study. *Langmuir* **2004**, *20*, 3933−3939.
(19) Pilsl, H.; Hoffmann, H.; Hoffmann, S.; Kalus, J.; Kencono, A. W.; Lindner, P.; Ulbricht, W. Shape investigation of mixed micelles by small angle neutron scattering. *J. Phys. Chem.* **1993**, *97*, 2745−2754.
(20) Bergström, M.; Pedersen, J. S. Formation of tablet-shaped and ribbonlike micelles in mixtures of an anionic and a cationic surfactant. *Langmuir* **1999**, *15*, 2250−2253.
(21) Bergström, M.; Pedersen, J. S. A small-angle neutron scattering study of surfactant aggregates formed in aqueous mixtures of sodium dodecyl sulfate and didodecyldimethylammonium bromide. *J. Phys. Chem. B* **2000**, *104*, 4155−4163.
(22) Bergström, L. M.; Skoglund, S.; Danerlöv, K.; Garamus, V. M.; Pedersen, J. S. The growth of micelles, and the transition to bilayers, in mixtures of a single-chain and a double-chain cationic surfactant investigated with small-angle neutron scattering. *Soft Matter* **2011**, *7*, 10935−10944.
(23) Bergström, L. M.; Garamus, V. M. Structural behaviour of mixed cationic surfactant micelles: A small-angle neutron scattering study. *J. Colloid Interface Sci.* **2012**, DOI: 10.1016/j.jcis.2012.05.015, in press.
(24) De, S.; Aswal, V. K.; Goyal, P. S.; Bhattacharya, S. Characterization of new Gemini surfactant micelles with phosphate headgroups by SANS and fluorescence spectroscopy. *Chem. Phys. Lett.* **1999**, *303*, 295−303.
(25) Aswal, V. K.; De, S.; Goyal, P. S.; Bhattacharya, S.; Heenan, R. K. Micellar structures of dimeric surfactants with phosphate head groups and wettable spacers: A small-angle neutron scattering study. *Phys. Rev. A* **1999**, *59*, 3116−3122.
(26) Alami, E.; Abrahmsén-Alami, S.; Eastoe, J. Investigation of microstructure and dynamics of novel Gemini surfactant micelles by small-angle neutron scattering (SANS) and NMR self-diffusion. *Langmuir* **2003**, *19*, 18−23.
(27) Hirata, H.; Hattori, N.; Ishida, M.; Okabayashi, H.; Frusaka, M.; Zana, R. Small-angle neutron-scattering study of bis(quaternary ammonium bromide) surfactant micelles in water. Effect of the spacer chain length on micellar structure. *J. Phys. Chem.* **1995**, *99*, 17778−17784.
(28) Aswal, V. K.; De, S.; Goyal, P. S.; Bhattacharya, S.; Heenan, R. K. Small-angle neutron scattering study of micellar structures of dimeric surfactants. *Phys. Rev. A* **1998**, *57*, 776−783.
(29) De, S.; Aswal, V. K.; Goyal, P. S.; Bhattacharya, S. Novel Gemini micelles from dimeric surfactants with oxyethylene spacer chain. Small angle neutron scattering and fluorescence studies. *J. Phys. Chem. B* **1998**, *102*, 6152−6160.
(30) Bowers, J.; Danks, M. J.; Bruce, D. W.; Heenan, R. K. Surface and aggregation behavior of aqueous solutions of Ru(II) metallosurfactants: 1. Micellization of [Ru(bipy)2(bipy¢)][Cl]2 complexes. *Langmuir* **2003**, *19*, 292−298.
(31) Borse, M.; Sharma, V.; Aswal, V. K.; Pokhriyal, N. K.; Joshi, J. V.; Goyal, P. S.; Devi, S. Small angle neutron scattering and viscosity studies of micellar solutions of bis-cationic surfactants containing hydroxyethyl methyl quaternary ammonium head groups. *Phys. Chem. Chem. Phys.* **2004**, *6*, 3508−3514.
(32) Borse, M.; Sharma, V.; Aswal, V. K.; Goyal, P. S.; Devi, S. Aggregation properties of mixed surfactant systems of dimeric butane-1,4-bis(dodecylhydroxyethylmethylammonium bromide) and its monomeric counterpart. *Colloids Surf. A* **2006**, *287*, 163−169.
(33) FitzGerald, P. A.; Davey, T. W.; Warr, G. G. Micellar structure in Gemini nonionic surfactants from small-angle neutron scattering. *Langmuir* **2005**, *21*, 7121−7128.
(34) Nieh, M.-P.; Kumar, S. K.; Fernando, R. H.; Colby, R. H.; Katsaras, J. Effect of the hydrophilic size on the structural phases of aqueous nonionic Gemini surfactant solutions. *Langmuir* **2004**, *20*, 9061−9068.
(35) Borse, M. S.; Devi, S. Importance of head group polarity in controlling aggregation properties of cationic gemini surfactants. *Adv. Colloid Interface Sci.* **2006**, *123*−*126*, 387−399.
(36) Aswal, V. K.; Haldar, J.; De, S.; Goyal, P. S.; Bhattacharya, S. Characterization of vesicles from ion-paired Gemini surfactants by small angle neutron scattering. *Phys. Chem. Chem. Phys.* **2003**, *5*, 907−910.
(37) Knaebel, A.; Oda, R.; Mendes, E.; Candau, S. J. Lamellar structures in aqueous solutions of a dimeric surfactant. *Langmuir* **2000**, *16*, 2489−2494.
(38) Fielden, M.; Claesson, P. M.; Verall, R. E. Investigating the adsorption of the Gemini surfactant "12−2-12" onto mica using

atomic force microscopy and surface force apparatus measurements. *Langmuir* **1999**, *15*, 3924−3934.
(39) Cotton, J. P. Initial data treatment. In *Neutron, X-Ray and Light Scattering: Introduction to an Investigative Tool For Colloidal and Polymeric Systems*; Lindner, P., Zemb, T., Eds.; North-Holland: Amsterdam, 1991; pp 19−31.
(40) Wignall, G. D.; Bates, F. S. Absolute calibration of small-angle neutron scattering data. *J. Appl. Crystallogr.* **1987**, *20*, 28−39.
(41) Pedersen, J. S. Analysis of small-angle scattering data from colloids and polymer solutions: Modeling and least-squares fitting. Adv. *Colloid Interface Sci.* **1997**, *70*, 171−210.
(42) Pedersen, J. S. Resolution effects and analysis of small-angle neutron scattering data. *J. Phys. IV (Paris) Coll. C8* **1993**, *3*, 491−498.
(43) Pedersen, J. S.; Posselt, D.; Mortensen, K. Analytical treatment of the resolution function for small-angle scattering. *J. Appl. Crystallogr.* **1990**, *23*, 321−333.
(44) Chevalier, Y.; Zemb, T. The structure of micelles and microemulsions. *Rep. Prog. Phys.* **1990**, *53*, 279−371.
(45) Corkill, J. M.; Goodman, J. M.; Walker, T. Partial molar volumes of surface-active agents in aqueous solution. *Trans. Faraday Soc.* **1967**, *63*, 768−772.
(46) Cabani, S.; Gianni, P.; Mollica, V.; Lepori, L. Group contributions to the thermodynamic properties of non-ionic organic solutes in dilute aqueous solution. *J. Solution Chem.* **1981**, *10*, 563−593.
(47) Aratono, M.; Onimaru, N.; Yoshikai, Y.; Shigehisa, M.; Koga, I.; Wongwailikhit, K.; Ohta, A.; Takiue, T.; Lhoussaine, B.; Strey, R.; Takata, Y.; Villeneuve, M.; Matsubara, H. Spontaneous vesicle formation of single chain and double chain cationic surfactant mixtures. *J. Phys. Chem. B* **2007**, *111*, 107−115.
(48) Hayter, J. B.; Penfold, J. Determination of micelle structure and charge by neutron small-angle scattering. *Colloid Polym. Sci.* **1983**, *261*, 1027−1030.
(49) Kotlarchyk, M.; Chen, S. H. Analysis of small angle neutron scattering spectra from polydisperse interacting colloids. *J. Chem. Phys.* **1983**, *79*, 2461−2469.
(50) Mittelbach, P.; Porod, G. X-ray small-angle scattering of dilute colloidal systems. VII. Computations for scattering curves of triaxial ellipsoids. *Acta Phys. Austr.* **1962**, *15*, 122−147.
(51) Hayter, J. B.; Penfold, J. An analytic structure factor for macroion solutions. *Mol. Phys.* **1981**, *42*, 109−118.
(52) Hansen, J. P.; Hayter, J. B. A rescaled MSA structure factor for dilute charged colloidal dispersions. *Mol. Phys.* **1982**, *46*, 651−656.
(53) Guiner, A. La diffraction des rayons X aux tres petits angles; application a l'etude de phenomenes ultramicroscopiques. *Ann. Phys.* **1939**, *12*, 161−237.
(54) Bevington, B. R. *Data Reduction and Error Analysis for Physical Sciences*; McGraw-Hill: New York, 1969.
(55) Bergström, L. M. Thermodynamics of self-assembly. In *Application of Thermodynamics to Biological and Material Science*; Tadashi, M., Ed.; InTech: Rijeka, 2011; pp 289−314.
(56) Cabane, B.; Duplessiz, R.; Zemb, T. High resolution neutron scattering on ionic surfactant micelles: SDS in water. *J. Phys. (Paris)* **1985**, *46*, 2161−2179.
(57) Tanford, C. *The hydrophobic effect*; Wiley: New York, 1980.
(58) Hall, D. G.; Pethica, B. A. Thermodynamics of micelle formation. In *Nonionic Surfactants*; Schick, M. J., Ed.; Marcel Dekker: New York, 1967.
(59) Israelachvili, J. N.; Mitchell, D. J.; Ninham, B. W. Theory of self-assembly of hydrocarbon amphiphiles into micelles and bilayers. *J. Chem. Soc., Faraday Trans. 2* **1976**, *72*, 1525−1568.
(60) Israelachvili, J. N., *Intermolecular and Surface Forces*. 3rd ed.; Academic Press: New York, 2011.
(61) Helfrich, W. Elastic properties of lipid bilayers: Theory and possible experiments. *Z. Naturforsch. C* **1973**, *28*, 693−703.
(62) Bergström, L. M. Bending energetics of tablet-shaped micelles: A novel approach to rationalize micellar systems. *ChemPhysChem* **2007**, *8*, 462−472.
(63) Bergström, L. M. Bending elasticity of nonionic surfactant layers. *Langmuir* **2009**, *25*, 1949−1960.